

Supporting Information

Crosslinking of polymers from monofunctional acrylates via C–H bond activation

Junkyu Kim¹, Seokju Lee¹, Youngjoo Park¹, Woojin Jeon¹, and Min Sang Kwon^{1,*}

¹Department of Material Science and Engineering, Research Institute of Advanced Materials, Seoul National University, Seoul 08826, Republic of Korea

E-mail: minsang@snu.ac.kr

Contents

Supplementary Note 1. General information	3
1.1. Chemicals and materials	3
1.2. General experimental procedures	3
1.3. Instrumentation.....	4
Supplementary Note 2. The mechanistic pathways of radical generation.....	6
Supplementary Note 3. Chracterization of acrylic polymers.....	7
Supplementary Note 4. DFT calculation.....	10
Supporting Information references.....	13

Supplementary Note 1. General information

1.1. Chemicals and materials

The 4DP-IPN was synthesized following the procedures previously reported by our group.^{1,2} All chemicals and solvents used in the syntheses were purchased commercially (Aldrich, TCI, Alfa, and etc.) and were used as received, without further purification. Methyl acrylate (MA, Aldrich), butyl acrylate (BA, Aldrich), lauryl acrylate (LA, TCI), isobornyl acrylate (IBOA, Aldrich), 2-ethylhexyl acrylate (EHA, Aldrich), isononyl acrylate (INA, TCI), 2-hydroxyethyl acrylate (HEA, TCI), 4-hydroxybutyl acrylate (HBA, TCI), 2-methoxyethyl acrylate (MEA, Aldrich), 2-[2-(2-methoxyethoxy)ethoxy]ethyl acrylate (MEEEA, TCI), 1-hydroxycyclohexyl phenyl ketone (Irgacure 184, TCI), benzophenone (BP, Alfa), [4-(octyloxy)phenyl](phenyl)iodonium hexafluoroantimonate (HNu 254, TCI), 2-butanoyloxyethyl(trimethyl)azanium butyl(triphenyl)boranuide (Borate V, Spectra Group Limited, Inc.), and ethyl acetate (Alfa) were purchased commercially. Release film (silicon-treated PET film, 100 μm , youngwoo trading) was also purchased commercially. Monomers were purified by passing them through basic alumina (Aldrich) to remove inhibitors (monoethyl ether hydroquinone, MEHQ).

1.2. General experimental procedures

■ General experimental procedures for acrylic polymers (UV-cured)

Acrylic syrup. A 20 ml glass vial (Sungho SIGMA) equipped with a stirring bar was charged with a monomer mixture and photoinitiator (Irgacure 184 or benzophenone, 200 ppm). The vial was sealed with a rubber septum and parafilm, and 99.999% pure N_2 was bubbled through the mixture for 30 minutes. The acrylic syrup was then synthesized under UV (ultraviolet) light lamp ($\lambda_{\text{max}} = 365 \text{ nm}$, 25 mW/cm^2) at room temperature. The acrylic syrup was adjusted to achieve a conversion rate of 4 to 8%.

Acrylic film. After synthesizing the acrylic syrup, an additional 1600 ppm of photoinitiator (Irgacure 184 or benzophenone) was added to facilitate film curing. To proceed with the film curing process, the acrylic syrup was cast to a uniform thickness of 50 μm using an applicator between two release films. The UV light lamp ($\lambda_{\text{max}} = 365 \text{ nm}$, 10 mW/cm^2) was used for film curing.

Acrylic polymer solution. For solution polymerization, a 20 ml glass vial (Sungho SIGMA) equipped with a stirring bar was charged with a monomer mixture, Irgacure 184, and ethyl acetate (solvent). The vial was sealed with a rubber septum and parafilm, and 99.999% pure N_2 was bubbled through the mixture for 30 minutes. The acrylic polymer solution was then synthesized under UV light lamp ($\lambda_{\text{max}} = 365 \text{ nm}$, 25 mW/cm^2) at room temperature.

■ General experimental procedures for acrylic polymers (visible light-cured)

Acrylic syrup. A 20 ml glass vial (Sungho SIGMA) equipped with a stirring bar was charged with a monomer mixture, and photoinitiating system (PIS, 4DP-IPN (3 ppm), HNu 254 (1000

ppm), and Borate V (600 ppm)). The vial was sealed with a rubber septum and parafilm, and 99.999% pure N₂ was bubbled through the mixture for 30 minutes. The acrylic syrup was then synthesized under 3W MR 16 light-emitting diode (LED) ($\lambda_{\text{max}} = 455 \text{ nm}$, 25 mW/cm²) at room temperature. The acrylic syrup was adjusted to achieve a conversion rate of 4 to 8%.

Acrylic film. Two 15 W string-type blue LEDs ($\lambda_{\text{max}} = 452 \text{ nm}$, 10 mW/cm²) were used for film curing without additives. To proceed with the film curing process, the acrylic syrup was cast to a uniform thickness of 50 μm using an applicator between two release films.

1.3. Instrumentation

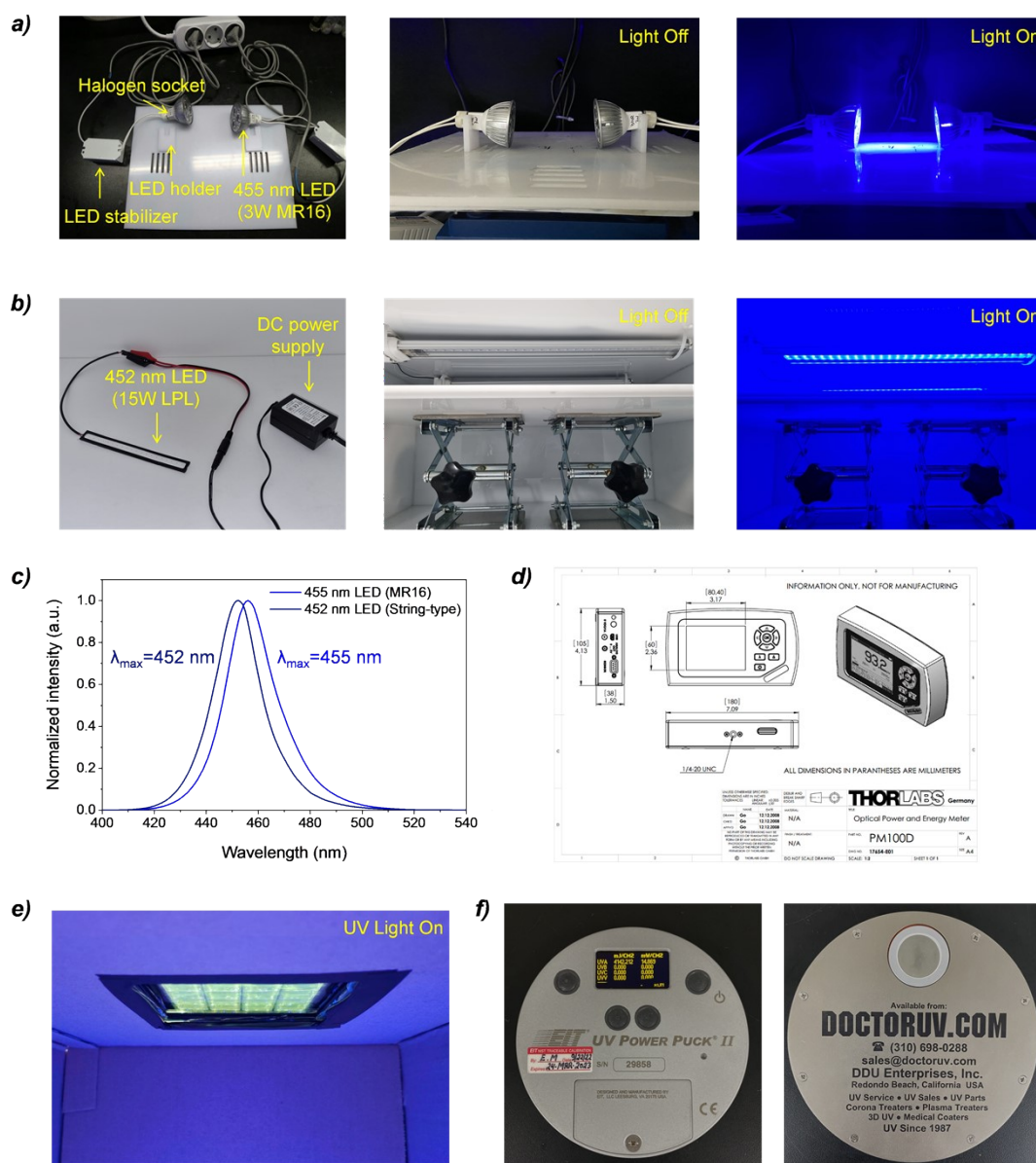


Fig S1. Experimental set-up for acrylic syrup and acrylic film curing. Blue LEDs for (a) acrylic syrup preparation and (b) film curing. (c) The emission spectra of the blue LEDs set-up. (d) An energy for evaluation of LED'S light intensity. (e) UV light lamp set-up for acrylic syrup preparation and film curing. (f) UVIcure plus II Power Puck to indicate the intensity of UV light lamp.

■ Fourier-transform infrared (FT-IR) spectroscopy measurements

FT-IR spectroscopy was conducted with Nicolet iS50 (Thermo Fisher Scientific) coupled with four position source mirrors (polaris long-lifetime mid-IR source, tungsten-halogen NIR/Vis source, raman InGaAs detector, focused emission port). And, three position detector mirrors (LN2 cooled, DLaTGS, RT), and attenuated total reflectance (ATR, iS50, all-reflective diamond ATR, mid- to far-IR capable: 80 to over 5000 cm^{-1} , pressure applied to 60 lbs). The conversion ratios of acrylic syrup and film were measured in ATR mode with scan number set to $n = 16$.

■ Gel permeation chromatography (GPC) measurements

Molecular weight of acrylic syrup and acrylic polymer solution was measured with SEC (Young In Chromass; YL9112 Plus isocratic pump) coupled with refractive index (RI) detector (YL9170 RI detector), Vacuum degasser (YL9101) and two different columns (Agilent Polypore 300×7.5 mm and Styragel HR5 300×7.8 mm in YL9130 column compartment).

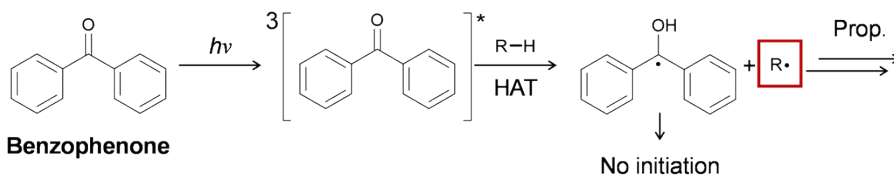
Supplementary Note 2. The mechanistic pathways of radical generation

■ Norrish type I photoinitiator



Irgacure 184

■ Norrish type II photoinitiator



Benzophenone

■ Photoinitiating system

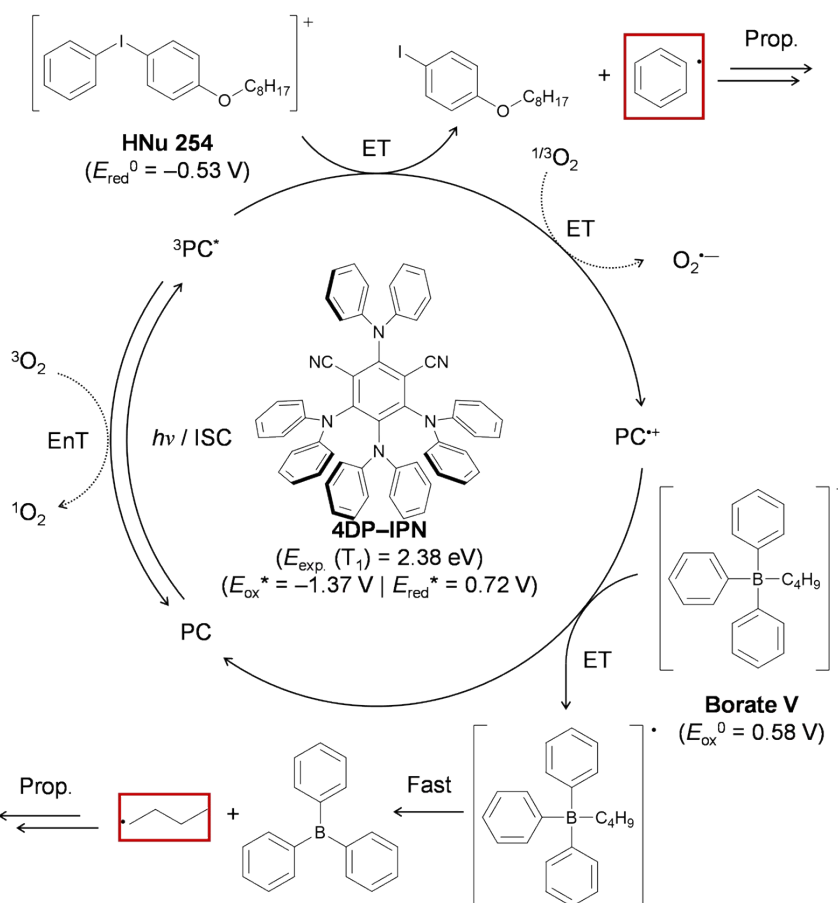


Fig S2. The mechanistic pathways of radical generation for each photoinitiators or PIS. Prop., ET, EnT, ISC indicate propagation, electron transfer, energy transfer, and intersystem crosslinking, respectively. The red squares denote an initiating radical that can polymerize.

Supplementary Note 3. Characterization of acrylic polymers

■ FT-IR analysis for polymer conversion estimation

The polymer conversion rate from FT-IR was calculated by following equation,

$$\text{Conversion (\%)} = \frac{\frac{A_{0(C=C)} - A_{t(C=C)}}{A_{0(C=O)}}}{\frac{A_{0(C=C)}}{A_{0(C=O)}}} \times 100$$

where, $A_{0(C=C)}$, $A_{0(C=O)}$, $A_{t(C=C)}$, and $A_{t(C=O)}$ represent the integrated areas of the characteristic peaks for C=C ($790\text{--}830\text{ cm}^{-1}$) and C=O ($1660\text{--}1760\text{ cm}^{-1}$) at the initial time, respectively. $A_{t(C=C)}$ and $A_{t(C=O)}$ indicate the integrated areas for these peaks at a later time t . If the integrated area is negative, the conversion is approximated to be 100%.

■ Determination of crosslinking ratio via gel content measurement

The insoluble fraction of cross-linked polymers was assessed through gel content measurement. Approximately 0.2 g of the polymer sample was dissolved in 30 ml of toluene at room temperature for 24 hours. While the linear portions of the sample completely dissolved, the crosslinked portions swelled. These crosslinked portions were then isolated using a steel mesh (#200, approximately $74\text{ }\mu\text{m}$) filtration. After filtration, the sample was dried under reduced pressure at 60°C for 24 hours. The gel content was determined using the following equation:

$$\text{Gel content (\%)} = \frac{W_{\text{filtered}}}{W_{\text{initial}}} \times 100$$

where, W_{initial} and W_{filtered} represent the weight of the polymer sample that initially dissolved in toluene and the weight of the cross-linked portion of sample.

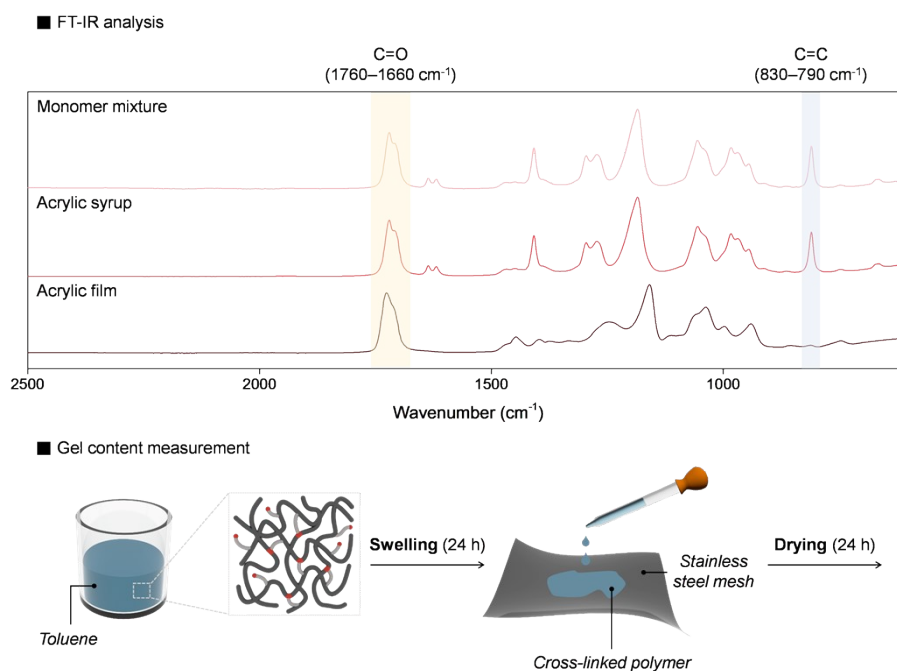


Fig S3. The FT-IR spectra for estimating polymer conversion and schematic diagram illustrating gel content measurement.

■ Experimental results of acrylic polymers

Table S1. The conversion and the number average molecular weight (M_n) of acrylic syrup polymerized using Irgacure 184. Notably, HEA and HBA remained insoluble in the solvent even in the acrylic syrup, hindering GPC measurement.

Entry	Monomer	Conversion _{acrylic syrup} (%)	M_n , acrylic syrup	PDI
1	MA	4.8	758.7	1.5
2	BA	5.0	1,281.6	1.47
3	LA	4.1	2,684.1	1.71
4	IBOA	4.6	1,001.7	1.46
5	EHA	6.2	2,082.3	1.69
6	INA	6.3	2,188.1	1.67
7	HEA	8.4	N.D. ^{a)}	N.D.
8	HBA	6.5	N.D.	N.D.
9	MEA	6.0	1,573.5	1.74
10	MEEEA	8.1	770.2	1.93

a) N.D. indicate not detected

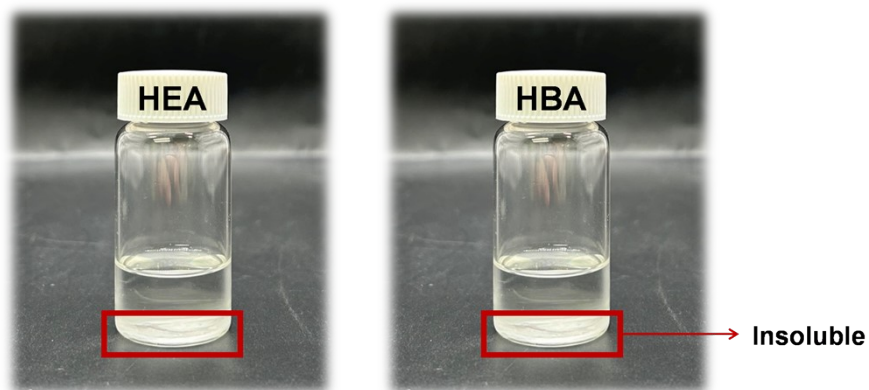


Fig S4. Photographic image showing HEA, and HBA homopolymer (acrylic syrup) that are insoluble in solvent.

Table S2. Variation in gel content with the proportion of crosslinkable monomers (HEA, HBA, and MEEEA) in copolymerization.

Entry	Monomer combination	Conversion _{acrylic syrup} (%)	Gel content (%)
1	HEA	8.4	97.9
2	[EHA] : [HEA] = 3 : 1	7.9	54.6
3	[EHA] : [HEA] = 3 : 2	5.5	80.6
4	[EHA] : [HEA] = 3 : 3	5.8	89.5
5	[EHA] : [HEA] = 3 : 4	6.1	95.1
6	HBA	6.5	98.6
7	[EHA] : [HBA] = 3 : 1	6.4	74.5
8	[EHA] : [HBA] = 3 : 2	6.1	91.3
9	[EHA] : [HBA] = 3 : 3	5.9	94.3
10	[EHA] : [HBA] = 3 : 4	5.8	97.4
11	MEEEA	8.1	97.1
12	[EHA] : [MEEEA] = 3 : 1	7.2	76.1
13	[EHA] : [MEEEA] = 3 : 2	7.1	92.4
14	[EHA] : [MEEEA] = 3 : 3	6.8	93.9
15	[EHA] : [MEEEA] = 3 : 4	6.4	96.5

Supplementary Note 4. DFT calculation

■ Density functional theory (DFT)

Density functional theory (DFT) calculation was performed with the B3LYP functional and 6–311++G(d) basis set with the Gaussian16 program package (Revision C.01 x86_64 AVX-enabled Binary Version). The geometries optimization, single point energies and oscillator strengths of vertical transition were calculated in ethyl acetate solution employing the polarizable continuum model (PCM). The Gibbs free energy and enthalpy with relevant standard state reference were obtained from following relations³, $G^0(298.15\text{ K}, 1\text{ M}) = G^{0*}(298.15\text{ K}, 1\text{ atm}) + 1.89\text{ kcal/mol}$ or $H^0(298.15\text{ K}, 1\text{ M}) = H^{0*}(298.15\text{ K}, 1\text{ atm}) + 0.59\text{ kcal/mol}$.

■ C–H bonds designated as H_donors for each monomer

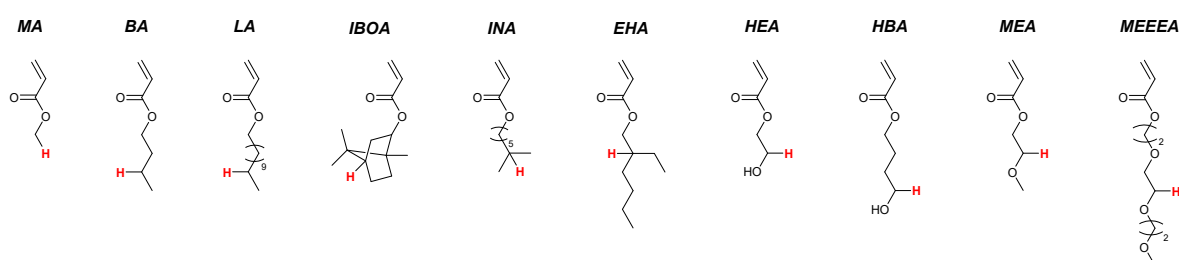


Fig S5. The position of the weakest C–H bond in the substituent of each monomer. We assumed the hydrogen at that location to be capable of undergoing HAT.

■ Detailed DFT calculation results

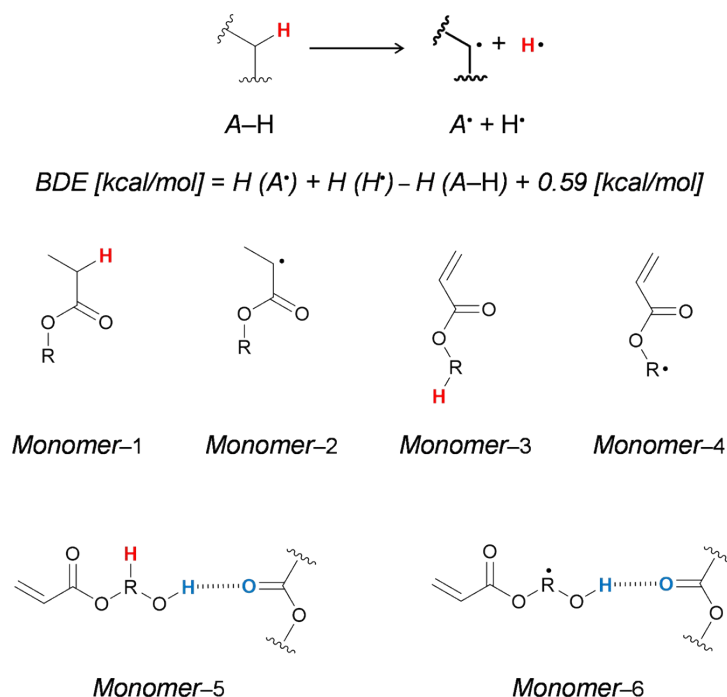


Fig S6. Calculation formula for bond dissociation enthalpy (BDE) and the molecular structures used for DFT calculations for each monomer. Specifically, to verify the changes in BDE due to hydrogen bonding, monomer-5

and monomer-6 were also included in the calculation.

Table S3. DFT calculation results (Gibbs free energy (G), and enthalpy (H)). Energies are given in hatree.

Entry	Monomer	G (Hatree)	H (Hatree)
1	MA-1	-307.707482	-307.667413
2	MA-2	-307.067123	-307.026677
3	MA-3	-306.495151	-306.457096
4	MA-4	-305.843513	-305.804662
5	BA-1	-425.600731	-425.548819
6	BA-2	-424.960127	-424.90809
7	BA-3	-424.387743	-424.338571
8	BA-4	-423.739081	-423.687898
9	LA-1	-739.968574	-739.886672
10	LA-2	-739.327582	-739.245928
11	LA-3	-738.755005	-738.67642
12	LA-4	-738.106906	-738.02624
13	IBOA-1	-580.389583	-580.335183
14	IBOA-2	-579.74931	-579.694453
15	IBOA-3	-579.177191	-579.125014
16	IBOA-4	-578.513803	-578.460973
17	EHA-1	-582.778143	-582.713718
18	EHA-2	-582.137527	-582.072933
19	EHA-3	-581.565531	-581.503465
20	EHA-4	-580.925128	-580.859277
21	INA-1	-582.782672	-582.717513
22	INA-2	-582.14246	-582.076751

23	INA-3	-581.570598	-581.507265
24	INA-4	-580.927395	-580.861087
25	HEA-1	-422.237716	-422.193163
26	HEA-2	-421.599125	-421.551514
27	HEA-3	-421.027031	-420.981823
28	HEA-4	-420.385083	-420.339686
29	HEA-5	-689.434395	-689.362668
30	HEA-6	-688.790572	-688.723034
31	HBA-1	-500.832176	-500.780557
32	HBA-2	-500.194305	-500.138893
33	HBA-3	-499.616077	-499.564699
34	HBA-4	-498.973581	-498.921217
35	HBA-5	-768.019676	-767.94434
36	HBA-6	-767.379003	-767.302932
37	MEA-1	-461.526867	-461.475676
38	MEA-2	-460.886548	-460.835029
39	MEA-3	-460.313166	-460.264459
40	MEA-4	-459.67312	-459.623252
41	MEEEA-1	-769.164832	-769.094842
42	MEEEA-2	-768.527403	-768.453234
43	MEEEA-3	-767.950907	-767.880962
44	MEEEA-4	-767.310337	-767.240016

Table S4. Comparison of activation energy results for propagation vs HAT. Energies are given in hatree.

Entry	Reaction	G_{reactant} (Hatree)	$G_{\text{transition state}}$ (Hatree)	G_{product} (Hatree)
1	Propagation	-842.626156	-842.59462	-842.628056

2	HAT (w/o hydrogen bonding)	-842.626156	-842.58372	-842.622799
3	HAT (w/ hydrogen bonding)	-1111.031928	-1110.990647	-1111.030486

■ Proposed crosslinking mechanism

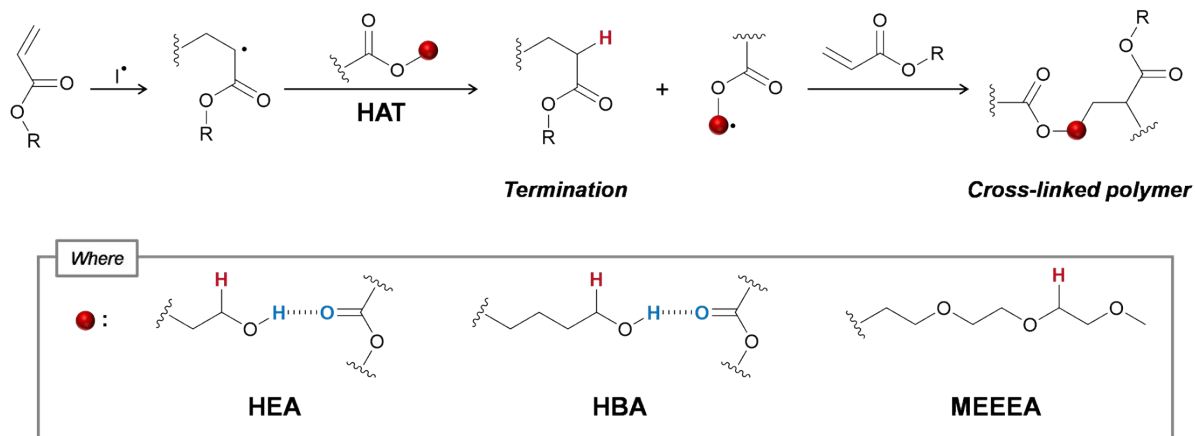


Fig S7. Schematic illustration of the proposed mechanism for cross-linked structure formation presented in this study.

Supporting information references

- 1 V. K. Singh, C. Yu, S. Badgajar, Y. Kim, Y. Kwon, D. Kim, J. Lee, T. Akhter, G. Thangavel, L. S. Park, J. Lee, P. C. Nandajan, R. Wannemacher, B. Milian-Medina, L. Luer, K. S. Kim J. Giershner, and M. S. Kwon, *Nat. Catal.*, 2018, **1**, 794-804.
- 2 W. Jeon, Y. Kwon, and M.S. Kwon, *Nat. Commun.*, 2024, **15**, 5160.
- 3 B. Thapa, and H. B. Schlegel, *J. Phys. Chem. A*, 2016, **120**, 5726-5735.